

# Focused Ion Beam Induced Nanodot, Nanocrystal and Nanofiber Growth

C. Schoendorfer, A. Lugstein, E. Bertagnoli

Vienna University of Technology, Department for Solid State Electronics,  
Floragasse 7, A-1040 Vienna, Austria

## Introduction

Ion beams focused to diameters in the range of several tens of nanometers offer an interesting opportunity for maskless processing in the nanoscale regime. Under certain sputter conditions a periodic height modulation in the form of ripples and dots on a submicron length scale develops during broad beam ion exposure as observed for semiconductor materials [1] – [4], metals [5], [6], insulator surfaces [7], and semimetals (e.g., graphite [8]). To gain full use of FIB techniques a fundamental understanding of the interaction of ion beams with the substrate material is required.

In this paper, we investigate the impact of FIB irradiation on GaAs, InAs, GaSb and Sb substrates and discuss the surface evolution. We will show, that under proper FIB adjustment of beam energy, beam diameter and beam current dots, crystals and fibers form due to selective etching and catalytic growth processes.

## Experimental

### Sample Preparation

In a twin lens FIB system  $\text{Ga}^+$  ions are extracted from a liquid Ga source, followed by acceleration up to 50 keV. The beam scanning in discrete steps across the sample surface leads to an ion bombardment of a defined area. Controlled FIB exposure of the sample is achieved by variation of some basic parameters such as the beam diameter, the beam current, the distance between two discrete steps along the scanning path and the dwell time which is the time the beam remains on each spot. The experiments are carried out with various ion fluences at normal incidence and at room temperature.

Our setup offers the possibility to image the focal plane during FIB processing. Therefore the surface evolution can be observed *in-situ* by FIB-SEM imaging. Furthermore, the nanopatterns are investigated by atomic force microscopy (AFM), Auger electron spectroscopy (AES), high resolution transmission electron microscopy (HRTEM) and X-ray diffraction.

### GaAs Substrates

The exposure of GaAs to the FIB leads to an excess of Ga on the substrate surface due to preferential sputtering of As [9]. Because of the surface tension the Ga agglomerates dots. Therefore, a formation of Ga-rich liquid droplets in the ion exposed area as shown in the SEM image in Fig. 1(a) can be observed. *In-situ* monitoring shows that these dots move around on the surface as long as this area is exposed to the FIB. Topography investigations by AFM have shown agglomeration of the droplets due to gathering at lower levels of the roughened surface which is displayed in Fig. 1(b). The

chemical composition of the dots has been analyzed by AES which confirmed that the droplets consist of nearly pure Ga.

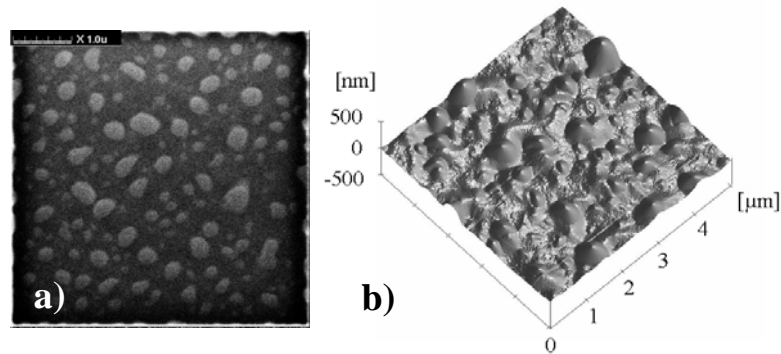


Fig. 1: (a) FIB-SEM image of a GaAs surface after FIB exposure of a 5  $\mu\text{m}$  x 5  $\mu\text{m}$  box with 50 keV Ga ions, (b) AFM topography of the GaAs sample after milling.

### InAs Substrates

Figure 2 shows SEM images of the InAs surface after 50 keV FIB exposure with different ion fluences. For an ion fluence of  $1.25 \times 10^{16}$  ions/cm<sup>2</sup> randomly distributed nano-grains are formed on the InAs surface (Fig. 2(a)). The extension size of these grains ranges from 30 to 120 nm and their typical number density is in the order of about  $2 \times 10^9$  cm<sup>-2</sup>. For an ion fluence of  $2.5 \times 10^{16}$  ions/cm<sup>2</sup> the size of the protrusions increases while the surface density decreases (Fig. 2(b)). For the highest investigated ion fluence of  $5 \times 10^{16}$  ions/cm<sup>2</sup> the grains grow further and emerge as well separated crystallites with obvious facets (Fig. 2(c)).

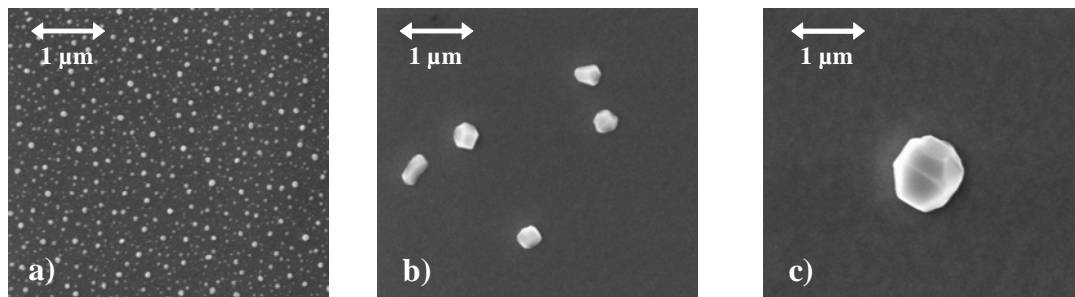


Fig. 2: Ion fluence dependency of pattern evolution on InAs exposed by the Ga FIB. The SEM images show the InAs surface after exposure fluences of (a)  $1.25 \times 10^{16}$  ions/cm<sup>2</sup>, (b)  $2.5 \times 10^{16}$  ions/cm<sup>2</sup> and (c)  $5 \times 10^{16}$  ions/cm<sup>2</sup>.

An explanation for this effect of an excess of In on the surface can be found in the different sputter rates of In and As. The mass difference implies that indium is sputter ejected at a much lower rate than arsenic which in addition to that is highly volatile when being in an atomic state. Due to this preferential sputtering of arsenic during FIB bombardment an excess of indium is formed on the exposed InAs surface. We assume that these excess indium atoms presumably diffuse on the ion-impacted surface, coalescing into islands or crystallites somewhere on the surface. To prove the assumption of In crystallite formation due to FIB exposure X-ray diffraction measurements are carried out, where the three most intense reflections of crystalline In are clearly visible.

Relative intensities and d spacings of these reflections are in good agreement with reference material [10].

### GaSb Substrates

The impact of the Ga FIB depositing different ion fluences on GaSb substrates can be retraced by the SEM images in Fig. 3. At the beginning of the exposure process beneath a thin surface layer a structure consisting of many hollow cells like a honeycomb is built. This is a result of the conglomeration of voids in the subsurface induced by the implanted Ga ions [11]. Ongoing milling leads to a transformation of the comb structure into a sponge-like network consisting of Ga and Sb in the same ratio including some Ga-rich precipitations on top of this fiber network. We assume that a catalytic growth process similar to the vapor-liquid-solid growth process [12] occurs, whereby the Ga droplets act as the needed catalytic particles.

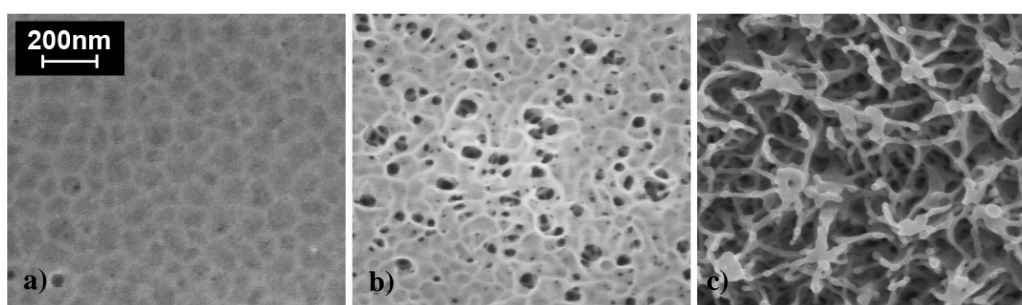


Fig. 3: GaSb surface evolution driven by ion fluence: depositing an ion fluence of  $3 \times 10^{13}$  ions/cm<sup>2</sup> (a) leads to generation of hollow combs under a thin surface layer, increasing the fluence to  $6 \times 10^{13}$  ions/cm<sup>2</sup> (b) results in a more and more porous layer and finally at an ion fluences of  $3 \times 10^{14}$  ions/cm<sup>2</sup> a transformation into a sponge-like network built up of GaSb fibers with diameter in the range of 25 nm and Ga-rich precipitations takes place.

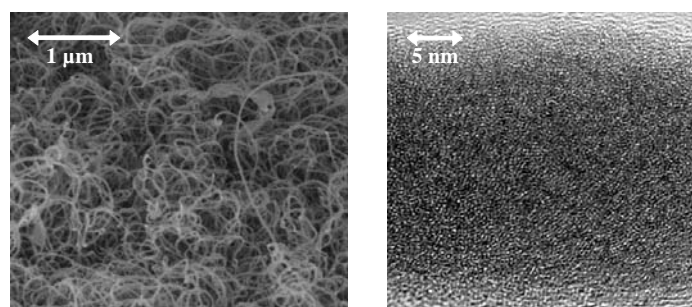


Fig. 4: The SEM image shows FIB generated Sb nanofibers with diameters in the order of 20 nm (a) and the HRTEM image of an individual Sb nanofiber proves that the as-grown nanofiber is completely amorphous even in the nanometer scale.

### Sb Substrates

The results of GaSb substrates exposed to the FIB lead to the idea that fibers growth could also occur using pure Sb as substrate. The catalyst material needed for the

growth may be provided by the focused Ga beam. In Fig. 4(a) a SEM image of an FIB milled box on metallic antimony using 50 keV Ga ions at an ion fluence of  $2 \times 10^{16}$  ions/cm<sup>2</sup> is given. The Sb nanofibers similar to those found on GaSb show diameters of few tens of nanometers and seem to grow in slopes beginning and ending at the substrate surface. HRTEM (Fig. 4 (b)) and AES investigations show that these fiber structures are completely amorphous and consist of pure Sb.

## Summary

In summary, investigation of FIB bombardment of several substrates is done. It is demonstrated that FIB parameters and the chemical composition of the substrates show a great influence on the surface evolution. Various effects which lead to different appearance in the sample surface evolution, such as Ga droplets on GaAs, In nanocrystals on InAs and nanowires with diameters in the range of few tens of nanometers on GaSb and metallic Sb, are studied by SEM and AFM. In addition to that the resulting nanostructures are investigated in detail using HRTEM, AES and XRD techniques to gain more information about the chemical composition and crystallographic structure. Thus, e.g. the In nanostructures can be considered to be crystalline and the as-grown Sb nanowires to be completely amorphous and to consist of pure Sb.

## Acknowledgements

This work is partly funded by the Austrian Science Fund (Project No. 18080-N07). The authors would like to thank the Center for Micro- and Nanostructures (ZMNS) for providing the clean-room facilities, Christian Tomastik for AES measurements and Johannes Bernardi for HRTEM investigations. The financial support from the Austrian Society for Micro- and Nanoelectronics (GMe) is gratefully acknowledged.

## References

- [1] E. Chason, T. M. Mayer, B. K. Kellerman, D. T. McIlroy, and A. J. Howard, *Phys. Rev. Lett.* 72, 3040 (1994).
- [2] G. Carter and V. Vishnyakov, *Phys. Rev. B* 54, 17647 (1996).
- [3] Z. X. Jiang and P. F. A. Alkemade, *Appl. Phys. Lett.* 73, 315 (1998).
- [4] J. Erlebacher, M. J. Aziz, E. Chason, M. B. Sinclair, and J. A. Floro, *Phys. Rev. Lett.* 82, 2330 (1999).
- [5] S. Rusponi, C. Boragno, and U. Valbusa, *Phys. Rev. Lett.* 78, 2795 (1997).
- [6] S. Rusponi, G. Costantini, C. Boragno, and U. Valbusa, *Phys. Rev. Lett.* 81, 4184 (1998).
- [7] T. M. Mayer, E. Chason, and A. J. Howard, *J. Appl. Phys.* 76, 1633 (1994).
- [8] S. Habenicht, W. Bolse, K. P. Lieb, K. Reimann, and U. Geyer, *Phys. Rev. B* 60, R2200 (1999).
- [9] J. G. Pellerin, D. P. Griffis, P. E. Russell, *J. Vac. Sci. Technol. B* 8, 1945 (1990).
- [10] The Powder Diffraction File, International Centre for Diffraction Data, 12 Campus Boulevard, Newton Square, Pennsylvania 19073-3273, USA.
- [11] N. Nitta, M. Taniwaki, Y. Hayashi, T. Yoshiie, *J. Appl. Phys.* 92, 1799 (2002).
- [12] R. S. Wagner, W. C. Ellis, *Appl. Phys. Lett.* 4, 89 (1964).